

# STRANGE ATTRACTORS IN THE SATURN RING SYSTEM

V. LALAJA, V. P. N. NAMPOORI, and R. PRATAP

*Department of Physics, Cochin University of Science and Technology, Cochin, India*

(Received 18 February, revised 16 July 1988)

**Abstract.** The three rings A, B and C of Saturn and the two gaps French and Cassini divisions in between them have been subjected to a study of deterministic chaos and we have shown the existence of spatially distributed strange attractors, implying thereby that the system is open, dissipative, nonequilibrium and non-Markovian in character.

Matter ring formation in the solar system in general (such as Asteroidal Belt) and in planetary environment (Galilian planets) in particular has still evaded adequate explanation. Various theories have been put forward based on Newtonian mechanics of three-body dynamics to explain the formation of gaps by gravitational collisional self focussing (Trulson, 1971), scavenging of matter by satellites involving resonance theory (Berry, 1978) with limited success. However, there seem to be only few attempts to analyse the data obtained by the various missions towards an understanding of the dynamics of these systems. In this paper, we propose to apply the recently developed theory of deterministic chaos (Schuster 1984) to the data acquired by the Voyager missions (photopolarimeter recordings; Esposito *et al.*, 1983). It may be mentioned that a study in the framework of deterministic chaos is relevant in the case of Saturn rings, in view of the results of Wisdom (1983) wherein he has shown that in asteroidal belt, 3:1 Kirkwood gap coincides with the outer boundary of a chaotic zone. The significance of 3:1 resonance out of all resonances was pointed out for the first time by Pratap (1977).

Our analysis in the present paper is *not* dependent on any particular Hamiltonian; and, hence, the dynamics that is imbedded in the actual data which become explicit here would enable one to frame a more realistic theory. The main results in this paper are that the system is in nonequilibrium state and is nonlinear and dissipative, and has only little information capacity as revealed by the low Kolmogorov entropy.

## Mathematical Analysis

The data set consists of the extinction data as recorded by the photopolarimeter in the Voyager mission from which the density distribution as a function of distance is obtained as given in Figure 1. This is recorded at an interval of 65 km ( $0.002R_s$ ) for a distance ranging from the inner edge of the innermost ring (C Ring) to the outer edge of A ring. The F ring and the gap between A and F are

*Earth, Moon, and Planets* 44: 105-119, 1989.

© 1989 Kluwer Academic Publishers. Printed in the Netherlands.

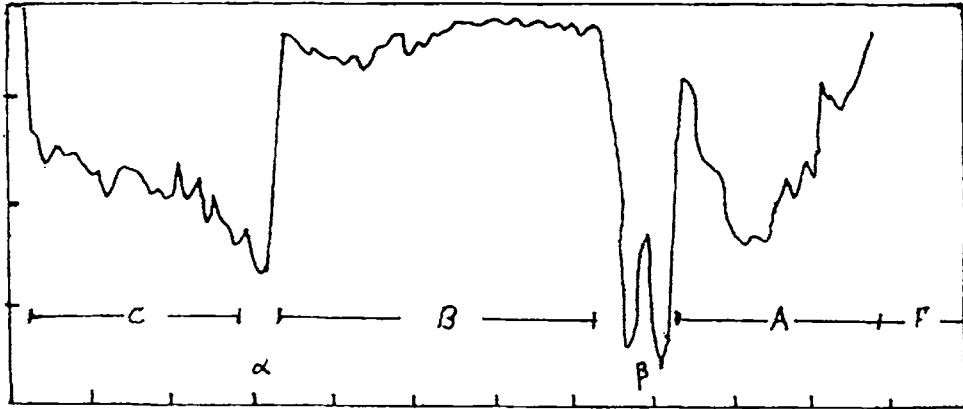


Fig. 1. Matter distribution as a function of radial distance from the inner edge of the C ring to the outer edge including F ring. We have considered in this analysis only from the inner edge of C to the outer edge of A ring.

not included in the present analysis, as also the D ring as is supposed to exist between the planet and the C ring. The distance is about  $1.03R_s$  and the division of the domain is given in Table I. These readings are given by the sequence

$$X(l) = X(l_0), X(l_0 + \Delta l), X(l_0 + 2\Delta l) \dots X(l_0 + N\Delta l), \tag{1}$$

where  $\Delta l$  is the distance gap between two consecutive readings. In the present case it is 65 km, and  $l_0$  is the innermost edge of the C ring. This sequence is now rearranged in the form of a 'delayed matrix' as

$$\begin{matrix} X(l_0) & X(l_0 + \Delta l) & X(l_0 + 2\Delta l) \dots & X(l_0 + m\Delta l), \\ X(l_0 + \Delta l) & X(l_0 + 2\Delta l) & X(l_0 + 3\Delta l) \dots & X(l_0 + (m + 1)\Delta l), \\ \dots & \dots & \dots & \dots \\ X(l_0 + d\Delta l) & X(l_0 + (d + 1)\Delta l) & X(l_0 + (d + 2)\Delta l) \dots & X(l_0 + (d + m)\Delta l). \end{matrix} \tag{2}$$

TABLE I

Table giving the summary of the present analysis

Ring/gap	In units of $R$		Width	$D_2$	$K_2 \times 10^3$
	Inner edge	Outer edge			
C	1.24	1.45	0.21	1.65	1.00
Gap	1.45	1.53	0.08	2.81	0.83
B	1.53	1.95	0.42	4.26	2.58
Gap	1.95	2.03	0.08	2.55	3.20
A	2.03	2.27	0.24	1.71	1.23
Total system	1.24	2.27	1.03	1.78	0.83

The matrix (2) is symmetric by construction and this need not necessarily be a square matrix. If  $N$  is even, then the above would be square matrix if  $m = d = N/2$ .

The matrix (2) can be considered as an array of  $m$  column vectors defined in a  $d$  dimensional space and this in general can be written as

$$\mathbf{X}_i = \{X(l_i), X(l_i + \Delta l), \dots X(l_i + d\Delta l)\}, \tag{3}$$

where  $l_i = l_0 + i\Delta l$  with  $i$  being an integer running from 0 to  $m$ . We shall now define a correlation function, following Atmanspacher and Scheingraber (1986) as

$$C_d(r) = \text{Lt}_{N \rightarrow \infty} \sum_{i,j=1}^N N^{-2} \Theta(r - \|\mathbf{X}_i - \mathbf{X}_j\|), \tag{4}$$

where  $r$  is any preassigned quantity and  $\|\cdot\|$  is the Euclidian norm of the difference between two vectors  $\mathbf{X}_i$  and  $\mathbf{X}_j$ .  $\Theta(x)$  is the Heaviside function which is unity for  $x > 0$  and zero for  $x < 0$ . Equation (4) gives the number of pairs of vectors whose difference is less than a preassigned  $r$  and normalised by  $N^2$ . The choice of  $r$  and  $d$  will become apparent in the sequel.

If we consider the trajectory of a particle crossing a given plane repeatedly, then if the points at which the trajectory crosses the plane are all confined in a neighbourhood, then this is called the basin of the attractor.  $r$  in Equation (4) gives a measure of the basin of the attractor. One can use the probability  $p_i (= N_i/N)$ , where  $N_i$  are the number of points at which a trajectory visits a given neighbourhood, to define quantities  $D_q$  which are called the  $q$ th order Hausdorff dimension of the attractor. This is elaborated in a series of papers by Grassberger and Procaccia (1983a, b and references quoted therein). The most significant of  $D_q$ s however is  $D_2$  which can be defined in terms of (4).

It has been shown by Grassberger and Procaccia (1983b) that for small  $r$ , Equation (4) obeys a power law as

$$C_d(r) \sim r^\epsilon, \tag{5}$$

which means that the points defined in (4) will all be in a hypercube of dimension  $\epsilon$  with sides  $r$ , and this correlation exponent  $\epsilon$  can be obtained as the slope of a linear relation

$$\log C_d(r) = \epsilon \log(r). \tag{6}$$

It has been shown that if the data set is generated from a completely stochastic Gaussian white noise, then  $\epsilon = d$  or a plot of slope against dimension would be a straight line making an angle of  $45^\circ$  with the dimension axis (Babloyntz and Destexhe, 1986). However, any deviation from this line would indicate the presence of a deterministic component. Thus the existence of a deterministic component in the data set can be uniquely determined without any recourse to the dynamical equations.

We can now define second order correlation dimension ( $q = 2$  in  $D_q$ ) by making (6) independent of  $r$  and  $d$ . We then have

$$D_2 = \text{Lt}_{\substack{r \rightarrow 0 \\ d \rightarrow \infty}} [\log C_d(r)/\log(r)], \quad (7)$$

and this quantity has been shown to be the lowest in the set of  $D_q$ s (Caputo and Atten, 1987). This is an invariant of the system and is a static parameter as it is independent of the length or time-scales. It may also be realised that the definition (7) holds good for a nonlinear dissipative system. This is the minimum number of initial conditions which are necessary to characterise the system in the asymptotic limit, or this gives the dimension of the subspace to which the system gets embedded in the phase space. As one can see in the discussion for the various domains, the curve slope- $d$ , takes off from zero and attains an asymptotic value parallel to the  $d$ -axis. Hence  $d$  should be chosen so as to get this asymptote defined properly.

A second point to be observed is the dimension  $d$  at which the curve meets the asymptote line. The part of the curve defined for lower dimension, indicate chaos while that at the asymptotic region represents order. Hence the dimension at which the curve meets the asymptote could denote the boundary between chaos and order. This is what has been observed by Wisdom (1983) and we verified this by a similar analysis and we obtained  $D_2 = 5$  meaning a regular attractor meeting the curve at  $d = 15$  thereby giving the 3:1 Kirkwood gap. This probably could be a significant point which has not been realised earlier, as no importance is attached to the dimension at which the asymptote meet the curve.

We can also define a second invariant quantity, the Kolmogorov entropy as

$$K_2 = \text{Lt}_{\substack{d \rightarrow \infty \\ r \rightarrow 0}} \tau^{-1} \log(C_d/C_{d+1}), \quad (8)$$

where  $\tau$  is the sampling interval.  $K_2 > 0$  is a sufficient condition for deterministic chaos, and hence can be used to quantify the degree of chaos. It should be realised that while  $D_2$  is a static parameter independent of time and length scales,  $K_2$  is a dynamic parameter very sensitive to scales in the system. We shall evaluate these quantities for the various parts of the ring and gap systems and are given in the next section. In the present analysis, we have used the method developed by Abraham *et al.* (1986) for small data sets. This has been used with great success in other fields (Lalaja *et al.*, 1987; Pratap *et al.*, 1987).

## Results

In the ensuing analysis we do not presuppose a Hamiltonian structure for the system or any other specific interaction. We shall present results in two different sets – of the rings as well as gaps. The last section is on the ring system taken as a

whole showing that it does not exhibit the various characteristics of the individual components. The fact that the system consists of a spatial distribution of a large number of strange attractors however can be inferred from the existence of plateaus in the slope vs dimension curve. The results are discussed in the last section. We have also indicated in this section the future direction in which this work will be continued.

#### C RING

This ring is the one closest to the planet that we are considering, and experience strong gravitational effect. The inner edge of this ring is at a radial distance of  $0.2R$ , from the planet's surface and has a width of  $0.21R$ , or  $1.3 \times 10^4$  km. Figure 2(i) gives the plot of  $\log C_d(r)$  vs  $\log(r)$  for the various dimensions  $d$ , the left hand side outermost is of dimension 1 and we evaluated upto 30 dimensions. In the figure, we have given about 25 dimensions to avoid overcrowding. The curve  $d=1$  has some structure, but as  $d$  increases, these structures disappear even though some small wobbles do persist. Such wobbles do not appear in other dynamical systems such as neural networks (Lalaja *et al.*, 1987) and, hence, does not seem to be an artifact due to smaller data set. We measure the slope of each curve and plot it against the dimension in Figure 2(ii)a. The curve attains a saturation value of 1.65. In this figure we have drawn a line (b) at  $45^\circ$  to the

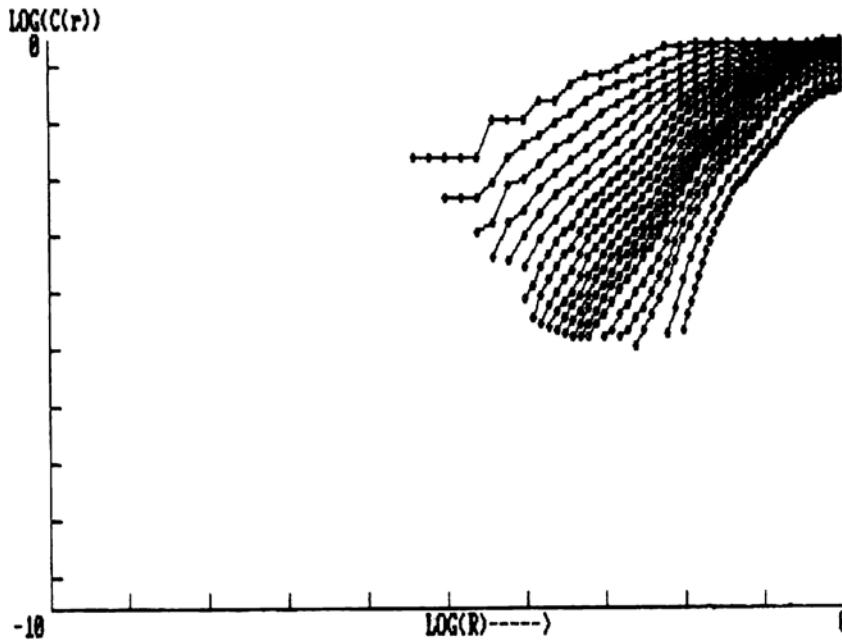


Fig. 2(i). Plot of  $\log C_d(r)$  against  $\log(r)$  for C ring. In this  $r$  is not the radial distance, but the parameter introduced in Equation (1).

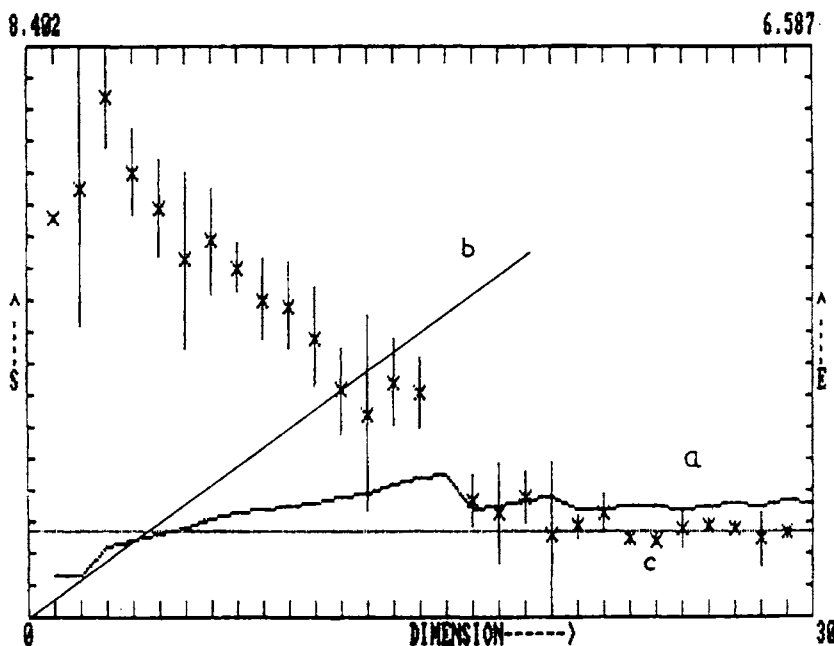


Fig. 2(ii). The plot gives three curves: slope vs dimension  $d$  (a) for the curves in Figure 2(i) the same for a completely stochastic case (b) and the plot of points  $K_2$  against  $d$ , (c). The asymptote is given by the straight line.

X-axis along which all the points would lie if the process is totally stochastic. Hence the deviation from this line indicates the existence of a deterministic part. The initial points for small dimensions indicate the noise component, while the asymptotic value gives the characteristic dimension of the attractor. The non-integer characteristic dimension indicates the existence of a strange attractor. The points we have plotted give the second Kolmogorov entropy – the most important component in the family of Kolmogorov entropies (Caputo and Atten, 1987). The line (c) drawn in the Figure 2(ii) is the asymptotic value of  $K_2$ . It may be mentioned that  $K_2$  is a sensitive parameter while  $D_2$  is a static parameter. Hence, the presence of multiple frequencies and length scales in the system would get reflected in this.

#### B RING

It may be noted that the  $\log C_d(r)$  vs  $\log(r)$  do not show much of wobbles for the initial dimensions, but starts appearing in the higher dimensions. We have evaluated correlations only upto  $r = 1$  and hence the curves do not converge to  $\log C_d(r) = 0$ . But the curves do converge to  $C_d(r) = 1$  if we take higher values of  $r$ . However we did not go for the same, since we need only the slopes and these do not change as  $r$  is increased beyond 1.

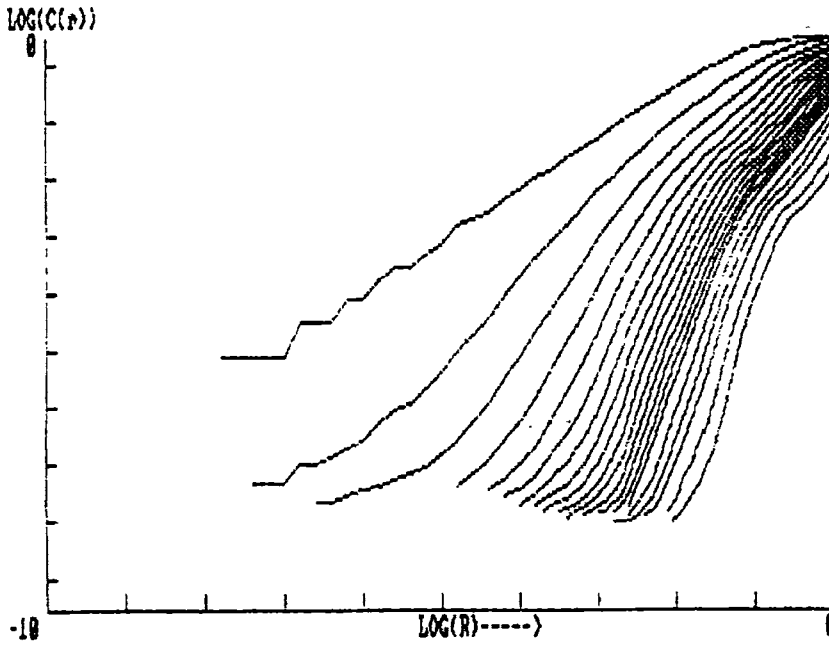


Fig. 3(i). Curves giving  $\log C_d(r)$  against  $\log(r)$  for B ring – the largest in the system.

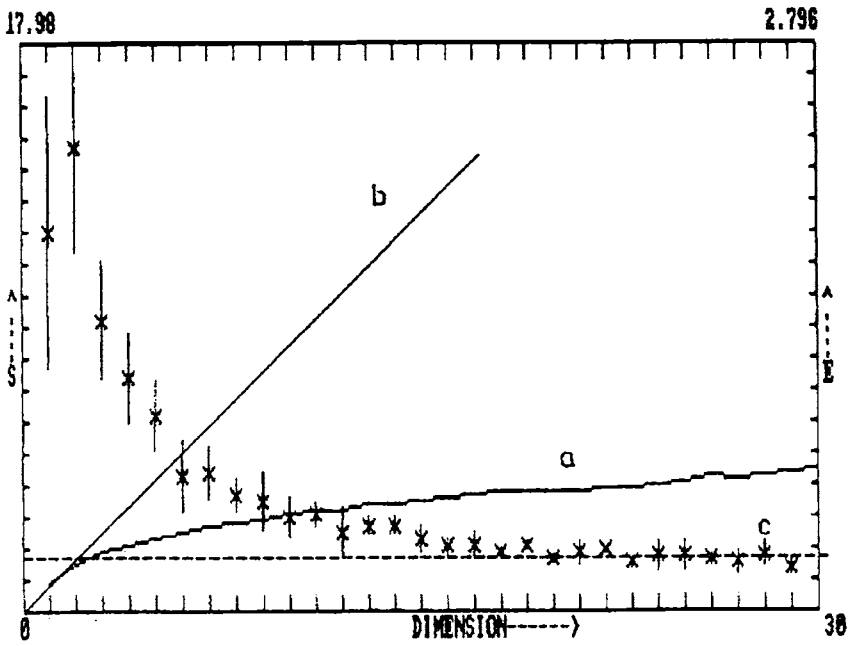


Fig. 3(ii). For the curves given in 3(i), the slope is plotted against  $d$  (a) the stochastic case (b), and the  $K_2$  entropy (c).

It may be mentioned that Figure 3(ii)a does show plateaus indicating the presence of more than one basin of attractors and if we take the mean of this, we get the characteristic dimension as 4.26. The asymptotic value of  $K_2$  given by Figure 3(ii)c however is well defined and gives the value 2.58.

#### A RING

This is the outermost ring we have considered here and experience less of gravitational force, as compared to others. The Voyager, however, observed knots and kinks in this ring system as well as concentric ring structures within the system. In the curves  $\log C_d(r)$  vs  $\log(r)$ , structures start appearing from the smaller dimensions onwards as is evident in Figure 4(i). These structures are indeed real and shows that there are more than one strange attractor in the system. To separate the various components however would be difficult and shall be looked into later on. This also became obvious in the slope vs dimension. As  $d$  increases, the attainment of the asymptotic value is slow. This is given in Figure 4(ii)a, and this implies that the deviation from the stochastic line (b) is slow. This is also apparent in the  $K_2$  entropy plot in Figure 4(ii)c wherein there exists oscillatory character, which dies down as  $d$  increases. Probably one can get an asymptotic value  $D_2$  for larger dimension. The existence of more than one attractor (regular or strange) in the system is quite apparent. It has a  $D_2$  value of about 1.71 and  $K_2 \sim 1.23$ . These values, are however, only tentative.

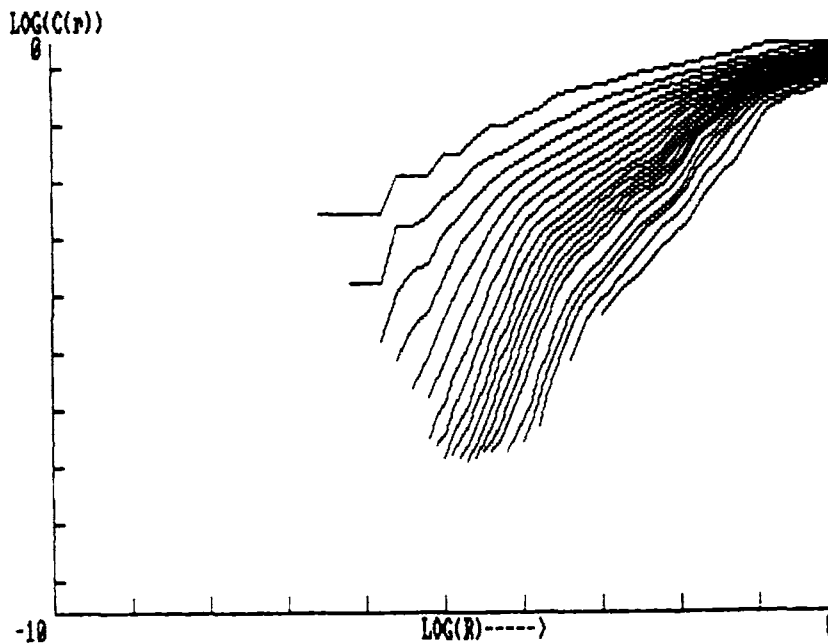


Fig. 4(i). Graph depicting  $\log C_d(r)$  vs  $\log(r)$  for A ring – the outermost one considered here.

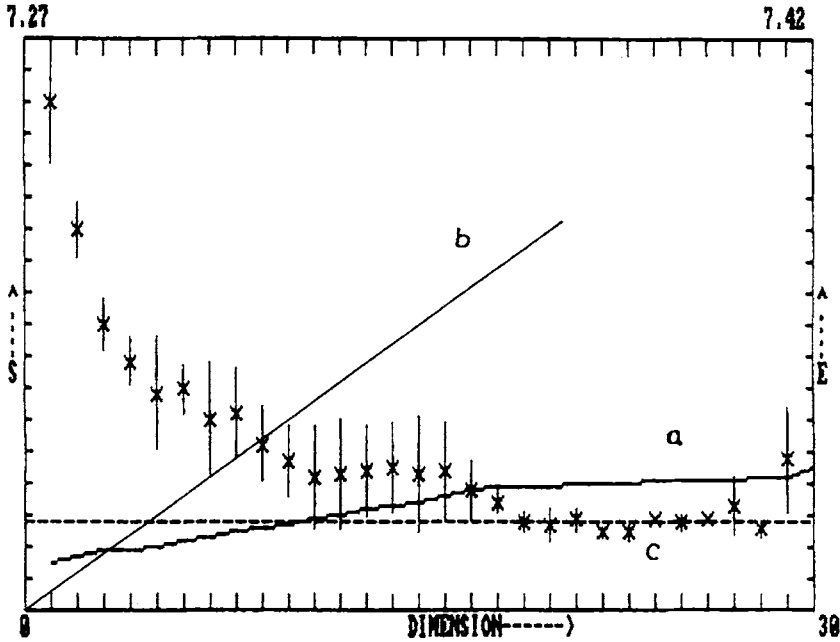


Fig. 4(ii). The plot of slope from 4(i) against  $d$  (a), and  $K_2$  vs  $d$  (c). (b) gives the completely stochastic case.

### Gaps

We shall carry out a similar analysis for the two gaps – between C and B rings (French division) and B gap – between B and A rings (Cassini division).

#### C GAP

The curve  $\log C_d(r)$  vs  $\log(r)$  for this region is given in Figure 5(i). A regular structure in the curve starts appearing right from the first dimension onwards, and as  $d$  increases, the step like structure also become more and more dominant. This manifests itself in a peculiar manner in the slope vs dimension Figure 5(ii)a. There does not exist a clear-cut asymptote, nor are the points along the stochastic line (b). The curve could be considered as a combination of large number of step curves, which shows the presence of more than one attractor. This is also evident from the  $K_2$  points distribution where these points exhibit a complicated oscillatory structure Figure 5(ii)c.

#### B GAP

Unlike the C gap, B gap or Cassini division is better structurewise. Structures start appearing as dimension increases and here again, the curves converge to unit correlation for large  $r$ . This is given in Figure 6(i). The curve in Figure 6(ii)a

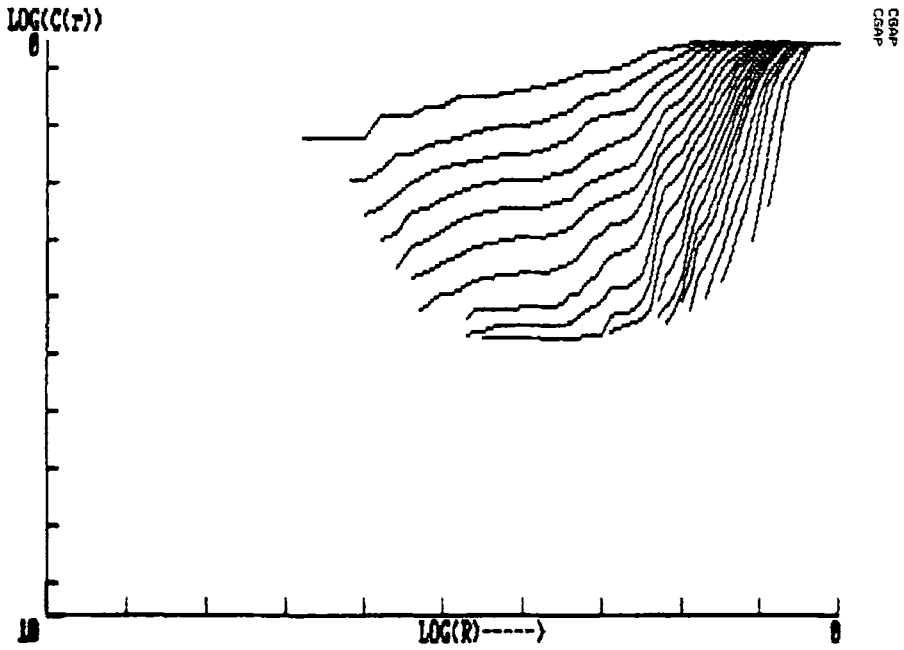


Fig. 5(i).  $\log C_d(r)$  vs  $\log(r)$  for the French Division or C Gap.

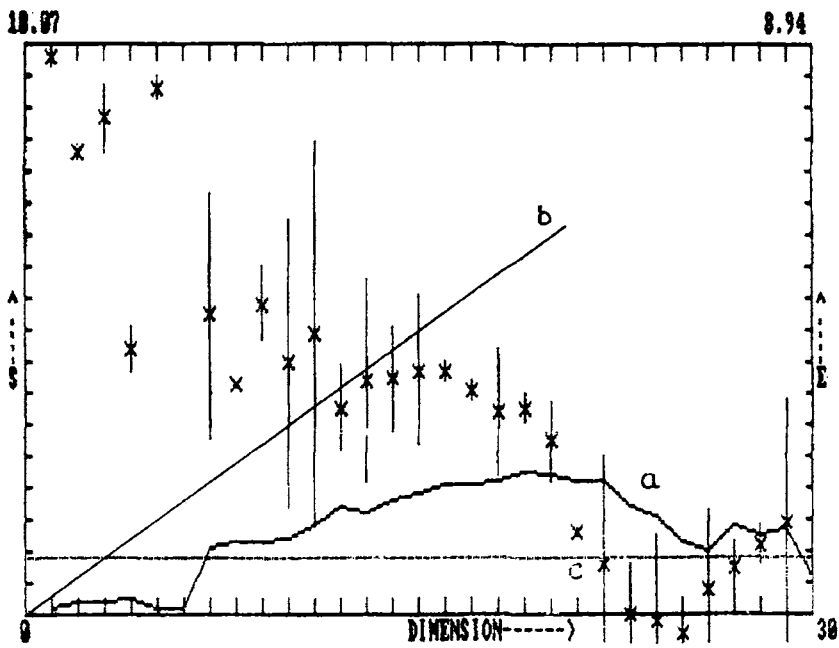


Fig. 5(ii). Slope derived from 5(i) against  $d$  (a), and  $K_2$  against  $d$  (c).

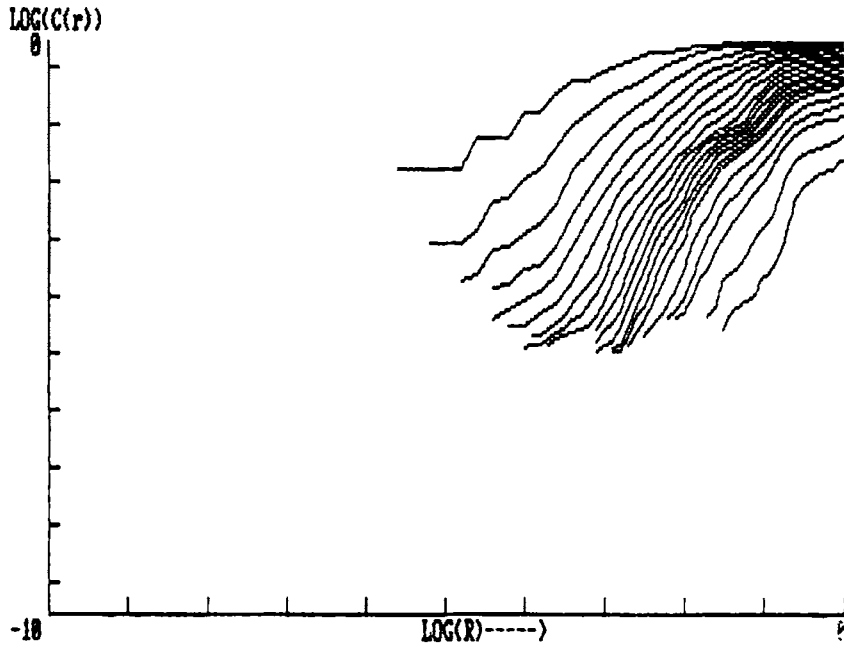


Fig. 6(i).  $\log C_d(r)$  is plotted against  $\log(r)$  for the Cassini Division or B Gap.

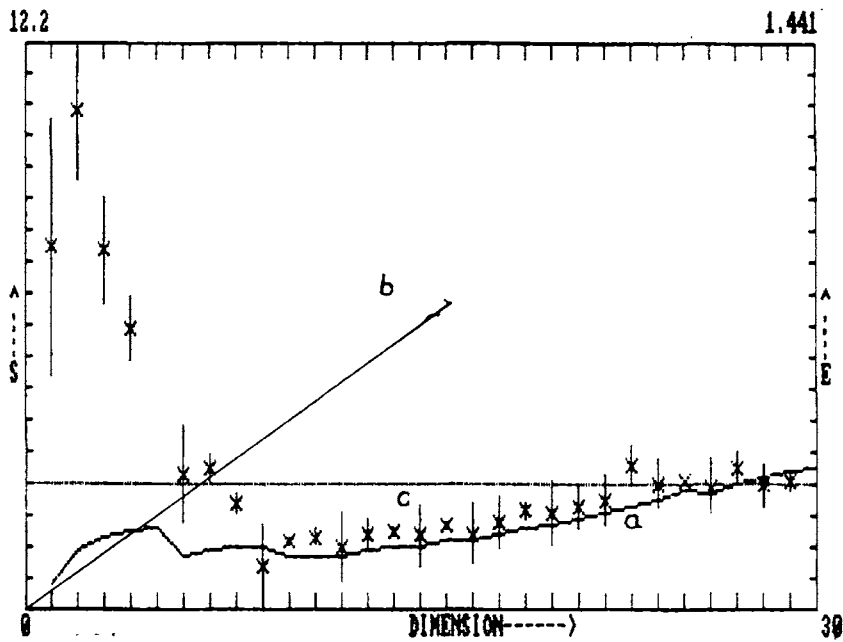


Fig. 6(ii). Slope vs.  $d$  (a) and  $K_2$  vs  $d$  for the Cassini Division. The stochastic line is given by the line b.

however do not show any sign of convergence in the asymptotic limit for the number of dimensions we have taken here. One does require a large number of dimensions which implies a larger number of closer data. The curve shows horizontal portions for dimension around 10, but takes off as dimensions go beyond 20. The curve 6(ii)c depicting the Kolmogorov entropy also exhibit a peculiar behaviour. It does show a saturation beyond dimension 20.

### Ring System as a Whole

Figure 7(i) gives the correlation curve for the entire ring system, for a range of  $1.03 R_s$  or about 62 000 km. As one can easily realise, the curve is not a sum of the previous ones, but has a different structure. There are pronounced wobbles in the diagram, implying distinct domains having different slopes. This manifests itself in the formation of plateaus in the various dimension ranges. Figure 7(ii)a, clearly implies the presence of various attractors having different characteristic dimensions. This is also quite evident from the fact that the deviation from the stochastic curve Figure 7(ii)b is also very clearly pronounced. In the plot for  $K_2$  Figure 7(ii)c, the ratio  $\log[C_d(r)/C_{d+1}(r)]$  oscillates for lower dimensions but steadies itself as  $d$  increases. It is however evident that one would not be able to get details of the earlier curves from this one. It has a characteristic dimension of 1.78 and a low  $K_2$  value of  $0.87 \times 10^{-3}$ .

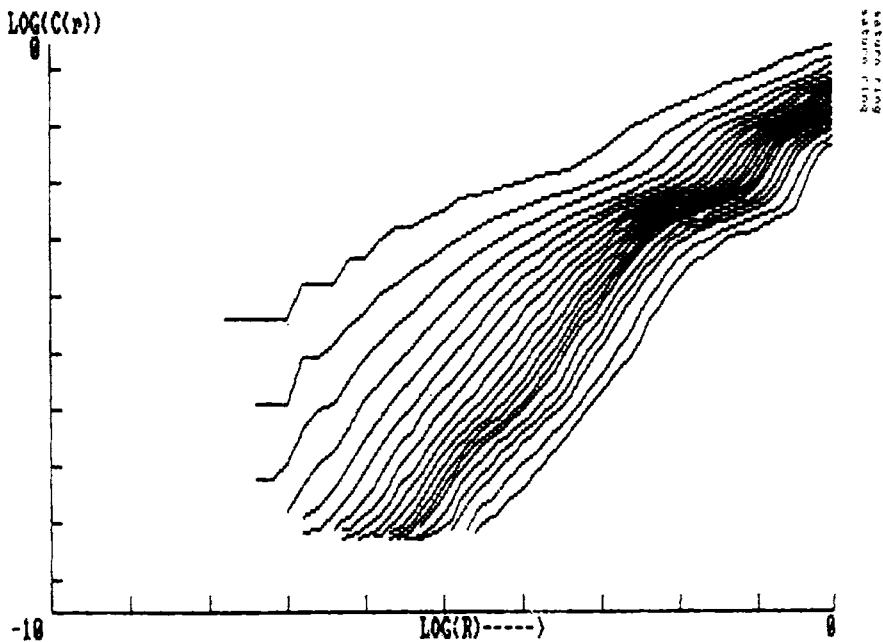


Fig. 7(i). The entire ring system from the inner edge of C to the outer edge of A is taken as a single unit and the  $\log C_d(r)$  vs  $\log(r)$  is plotted.

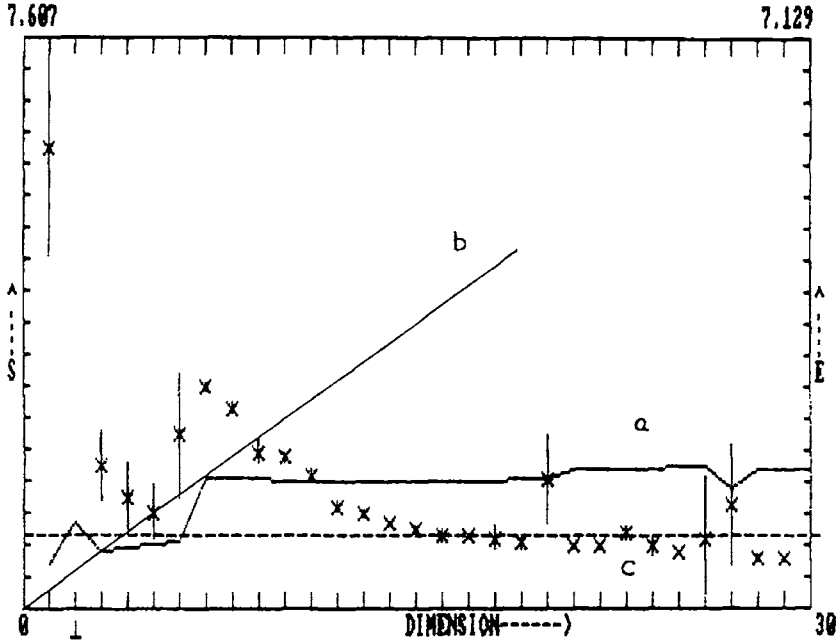


Fig. 7(ii). The slopes from 6(i) is plotted against dimension  $d$  (a)  $K_2$  against  $d$ (c).

**Conclusions**

The results of this analysis is given in Table I, and also in Figure 8. Some of the interesting features are that the characteristic dimension increases radially, comes to a maximum around the B ring and then shows a steady decrease, while  $K_2$  strikes a peak value around the Cassini gap and then decreases. This shows a phase lag between the dimension and the Kolmogorov entropy. An inspection of the dimensions reveal that all the attractors are strange and if we consider the total ring system, we get again a strange attractor. This is quite contrary to the result one obtains in the asteroidal belt wherein we get a regular attractor of dimension 5 for the system. We may conclude that the strange attractor for the total system is a consequence of a large number of interacting strange attractors, while if we extend this to the asteroidal system we can have a similar conclusion viz., a system of strange attractors resulting in the formation of a regular attractor. This implies that the Saturn ring system is chaotic piecewise as well as in total while in the asteroidal belt, the total system is a regular attractor, and is an example of chaos inducing order.

In this analysis, we followed a division of data based on density distribution. The main conclusion is that the Saturn rings form an open, dissipative, and non Markovian system consisting of more than one characteristic scale, manifesting

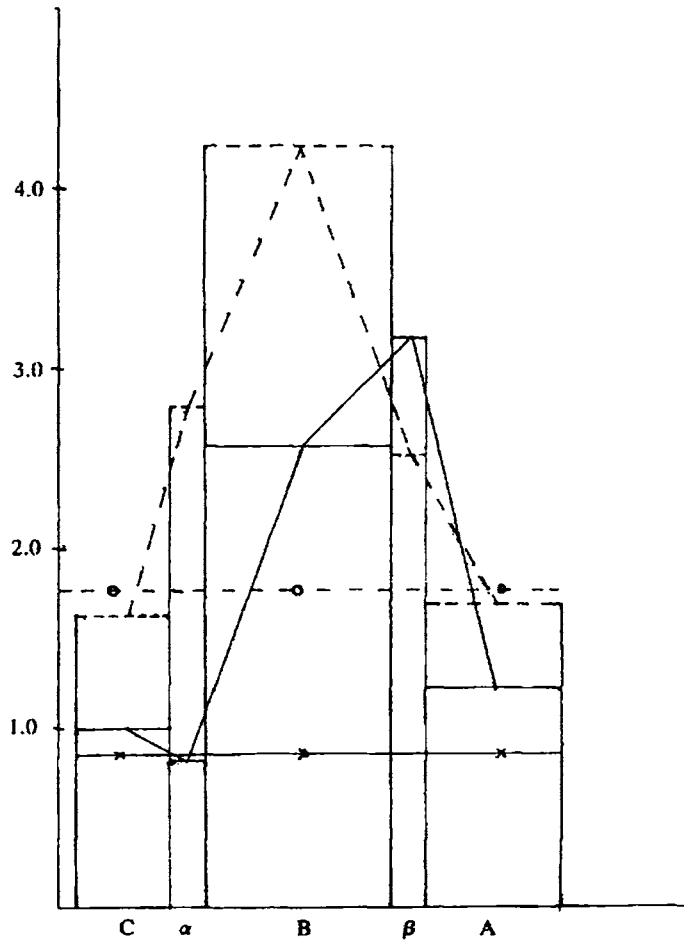


Fig. 8. The results given in the table is plotted against distance from the surface of the planet. This reveals the relation (if any) between  $D_2$  and  $10^3 K_2$ . Here the solid line is for  $K_2$  and the dashed line is for  $D_2$ .

itself in a collection of spatially distributed strange attractors (Schuster, 1984). Hence in developing a statistical mechanics of the system, it would be more realistic to consider a collection of strange attractors mutually interacting, giving rise to a resultant strange attractor or a regular one.

We are extending this by studying the autocorrelation of matter in these rings.

#### Acknowledgement

LV and RP would like to acknowledge financial support from Department of Science and Technology, Government of India through the grant 3(11)/82-STP 111.

### References

- Abraham, N. B., Albano, A. M., Das, B., De Guzman, G., Yang, S., Gioggia, R. S., Puccioni, G. P., and Tradice, J. R.: 1986, *Phys. Lett.* **114A**, 217.
- Atmanspacher, H. and Scheingraber, H.: 1986, *Phys. Rev. A* **34**, 254.
- Babloyantz, A. and Destexhe, A.: 1986, *Proc. Nat. Acad. Sci. (USA)* **83**, 3513.
- Berry, M. V.: 1978, 'Topics in Nonlinear Dynamics', *AIP Conf. Proc.* No. 46, 16.
- Caputo, J. G. and Atten, P.: 1987, *Phys. Rev. A* **35**, 1311.
- Esposito, L. W., O'Callaghan, M., Simmons, K. E., Hord, C. W., West, R. A., Lane, A. L., Pomphrey, R. B., Coffeen, D. L., and Sato, M.: 1983, *J. Geoph. Res.* **88**, 8643.
- Grassberger, P. and Procaccia, I.: 1983a, *Phys. Rev. Lett.* **50**(5), 346. 1983b, *Physica* **9D**, 189.
- Lalaja, V., Nampoori, V. P. N., and Pratap, R.: 1987, *Curr. Sci.* **56**, 1039. 1987b, Communicated to *Icarus*.
- Pratap, R.: 1977, *Pramana* **8**, 438.
- Pratap, R., Nampoori, V. P. N., and Lalaja, V.: 1987, *Intl. J. Neuro. Sci.* **39**, 245.
- Schuster, H. G.: 1984, *Deterministic Chaos*, Physik. Verlag GmbH D-6940 Weinheim, FRG.
- Trulsen, J.: 1971, 'Physical Studies of Minor Planets', T. Gehrels (ed.), NASA SP-267.
- Wisdom, J.: 1983, *Icarus* **56**, 51.